

In-plane seismic testing of precast concrete wall panels with grouted metal duct base connections

P. Seifi¹, R.S. Henry², and J.M. Ingham³

¹*Ph.D. Candidate, Dept. of Civil and Environmental Engineering, Univ. of Auckland. Auckland 1010, New Zealand (corresponding author). E-mail: psei698@aucklanduni.ac.nz*

²*Senior Lecturer, Dept. of Civil and Environmental Engineering, Univ. of Auckland. Auckland 1010, New Zealand. E-mail: rs.henry@auckland.ac.nz*

³*Professor, Dept. of Civil and Environmental Engineering, Univ. of Auckland. Auckland 1010, New Zealand. E-mail: j.ingham@auckland.ac.nz*

Abstract

In order to achieve satisfactory seismic performance, the connections between precast concrete wall panels and other structural elements should be well-designed to avoid brittle connection failure during an earthquake. Following the 2010/2011 Canterbury (New Zealand) earthquakes the seismic performance of grouted connections used for precast concrete wall panels was questioned. The brittle connection failure during the earthquake resulted in recommendations for more robust detailing of grouted metal duct connections. A set of experimental tests was performed to investigate the seismic behaviour of both existing and newly recommended detailing of precast concrete wall panels. Testing was comprised of seven full-scale precast concrete wall panels with wall-to-foundation grouted metal duct connections that were subjected to reversed cyclic in-plane lateral loading. Walls with existing connection detailing were found to perform adequately when carrying low axial loads, but performance was found to reduce as the axial load and wall panel length increased. The use of transverse confinement reinforcement around the grouted metal ducts was observed to prevent brittle connection response and to improve the robustness of the reinforcement splice.

Author keywords: Precast wall panels; Seismic design; Metal duct pull-out; Confinement; Energy dissipation.

26 INTRODUCTION

27 Precast concrete members are widely used in many countries for structural forms ranging from low-rise
28 warehouses to high-rise multi-storey buildings. In this form of construction, the structural concrete
29 components are cast off-site and are then assembled at the construction site. The advantages of utilizing
30 precast concrete elements are cost savings, better quality control, increased speed of construction,
31 reduced material consumption, and the potential to use high strength concrete (PCI 2010). Precast
32 concrete walls are commonly used as a primary force resisting system in a number of countries,
33 including US, Japan and New Zealand (Hawkins and Englekirk 1987), because of their significant
34 stiffness and strength against lateral forces deriving from earthquake and wind loads. The structural
35 behaviour of precast concrete walls is a combination of wall behaviour and connection behaviour
36 (rocking and base sliding) (Becker et al. 1980), with the contribution of connection behaviour on the
37 global seismic performance of the wall being dependent on the detailing of the connection and its
38 relative strength and stiffness.

39 One method that is used in New Zealand to connect precast concrete wall panels to their foundations
40 entails the use of metal duct grouted connectors, with an example of a metal duct connection shown in
41 Fig. 1a (Seifi et al. 2016). In this type of connection the starter bars from the foundation are positioned
42 inside metal ducts with a thickness of 0.3 mm that are cast inside the wall panel, and then the metal
43 ducts are filled with grout at the construction site, as shown in Fig. 1b. The main advantage of the metal
44 duct grouted connection is the simplicity of this detail, but the vulnerability of the connection detail was
45 revealed during the 2010/2011 Canterbury earthquakes (SESOC 2013). Fig. 2 shows an example of
46 metal duct connection damage during the 2010/2011 Canterbury earthquakes. To increase the seismic
47 robustness of the grouted connection between precast wall panels and the foundation, the Structural
48 Engineering Society of New Zealand (SESOC) has recommended new detailing for this connection
49 type (SESOC 2013). The proposed detailing requires that rectangular stirrups be used around ducts to
50 provide confinement for the connection and also to improve the robustness of the splice between the
51 connection and the vertical wall reinforcement, as shown in Fig. 3. It is generally accepted that
52 confinement improves the strength of the splices (Riva 2006).

53 In the present study seven precast concrete wall panels with conventional reinforcement detailing were
54 tested to verify the seismic performance of the panel-to-foundation connection when using grouted
55 metal ducts. The seismic performance of the wall panels is discussed, including details of load-
56 displacement behaviour, crack patterns, and wall-panel failure modes.

57 **BACKGROUND AND PREVIOUS RESEARCH**

58 The vulnerability of metal duct connections when used in precast concrete walls has been demonstrated
59 in several past studies (Riva et al. 2006; Kim 2000) and also during the 2010/2011 Canterbury
60 earthquakes in New Zealand (SESOC 2013). As an example, Crisafulli et al. (2002) tested a reinforced
61 concrete shear wall that was connected to its foundation using metal ducts, in order to evaluate the
62 seismic performance of walls having a lightly reinforced metal duct connection. The results of the
63 experiment indicated that the wall lateral stiffness decreased significantly at small lateral drifts, and
64 large residual displacements were measured during the experiment. In other research, the reversed
65 cyclic behaviour of columns connected to their foundation using grout filled metal ducts was compared
66 with the behaviour of cast-in-situ monolithic concrete columns (Kim 2000). It was found that the
67 grouted metal duct connection performed poorly due to deterioration of the longitudinal bar splice,
68 which caused reinforcement pull-out from the metal duct. Riva (2006) tested grouted-sleeve and
69 grouted-pocket column-to-foundation connections, and compared the behaviour of two precast concrete
70 columns having different connection types with the behaviour of cast-in-situ reinforced concrete
71 columns. Cyclic horizontal displacement was applied to the top of the columns to generate cyclic
72 moments at the column-to-foundation connection, and a constant axial load was applied. Although all
73 columns had almost the same flexural capacity, their energy dissipation and failure displacement were
74 different depending on the level of confinement provided to the connections, with enhanced ductility
75 and lower pinching observed in the connections that had a larger confinement level. It was established
76 that metal duct connections generally performed poorly as the column stiffness decreased due to the
77 formation of large cracks that spread around the metal ducts.

78 Contrary to the above studies where unfavourable behaviour was identified, several studies have been
79 undertaken where the use of metal duct connections has led to favourable behaviour being exhibited. A
80 comprehensive literature review on the behaviour of different types of connections used in bridge bent
81 caps was conducted by Restrepo et. al. (2011), where it was found that grouted metal duct connections
82 used in the bent cap had a linear behaviour that resulted in an extensive drift being achieved, with plastic
83 hinging forming in the column. Restrepo et. al. (2011) recommended that transverse joint shear
84 reinforcement be used to achieve full ductile behaviour of grouted metal duct connections.

85 The behaviour of an innovative grouted socket connection between cap beams and unbonded pre-
86 tensioned columns subjected to lateral seismic forces was examined by Thonstad et al (2016). It was
87 found that most damage occurred at the top and bottom of the column, and that the connection behaved
88 well with minimal damage experienced.

89 **PRECAST CONCRETE WALL SURVEY**

90 A review of detailing used in recently manufactured precast concrete wall panels was conducted by
91 collecting data from precast concrete manufacturers in three major New Zealand cities of Auckland,
92 Wellington and Christchurch. This review involved categorising more than 4800 wall panels used in
93 108 projects based upon geometry and reinforcement content of the wall panels, and the specific
94 characteristics of connections. Different detailing is used to connect precast concrete walls to their
95 foundations based on the type of structure and the magnitudes of the loads applied to the connection.
96 These connection types are generally based on one or a combination of the following three categories:
97 (1) dowel connections; (2) grouted connections; and (3) post-tensioned connections (Seifi et al. 2016).
98 The most commonly observed wall panel configuration, representing 42% of all walls, had a 150 mm
99 thickness and was reinforced with a single layer of vertical and horizontal bars. Double-layer reinforced
100 wall panels with a 200 mm thickness were documented in 25% of the reviewed detailing. The remaining
101 33% of wall panels had a thickness equal to or larger than 225 mm. The wall panel height to length
102 aspect ratio was observed to most commonly range between 3 and 5, and wall panels were typically
103 subjected to an axial load ranging from 0% to 10% $A_g f'_c$. Grade 500 MPa HD12 bars spaced at 250 mm

104 both horizontally and vertically was a common reinforcement detail. For panel-to-foundation metal duct
105 connections, the most commonly used reinforcing bar area was found to be between 0.4% and 0.6% of
106 the gross wall panel cross section, and the most commonly-used reinforcement was grade 500 MPa
107 HD16 with a spacing of 400 mm to 450 mm. The wall panels should be designed to have an inter-storey
108 drift of below 2.5% when subjected to the ultimate limit state (ULS) seismic force, based on
109 NZS 1170.5 (2004). However, it should also be noted that drift demands may exceed this limit during
110 a maximum considered earthquake, and that curvature limits for plastic hinge regions of different
111 ductility class in the New Zealand Concrete Structures Standard, NZS 3101:2006, will often govern the
112 design.

113 **EXPERIMENTAL PROGRAMME**

114 An experimental programme was developed to examine the seismic performance of precast concrete
115 wall panels with wall-to-foundation grouted metal duct connections. Different parameters such as
116 reinforcement details, wall panel thickness and aspect ratio, magnitude of axial load, and use of the
117 proposed confining stirrups were included in the experimental programme.

118 **Test specimen details**

119 The reinforcement and dimensions of the test wall panels were selected according to the most commonly
120 encountered details identified from the review exercise. All of the tested wall panels had a height to
121 length aspect ratio of between 2 and 3, which resulted in the dominant seismic response being associated
122 with rocking and flexural behaviour. The geometry and reinforcement details of the tested wall panels
123 and the applied axial load are summarised in Table 1. The first four wall panels represented perimeter
124 walls in industrial warehouse buildings, with a zero applied axial load and a height to length aspect ratio
125 of 3. These four wall panels represented panels from the perimeter wall of warehouse buildings where
126 the weight of the light steel roof is negligible in comparison to the selfweight of the precast concrete
127 wall panels. In Wall 1 no confining reinforcement was provided in the region of the panel-to-foundation
128 grouted metal duct connection, whereas Wall 2 and Wall 3 had the same geometry as for Wall 1 but
129 incorporated two different shapes of stirrups within the connection region. All wall panels except Wall

130 4 had a 150 mm thickness and vertical reinforcement as a single layer of HD12 (lower 5% characteristic
131 yield strength of 500 MPa) spaced at 225 mm, whilst Wall 4 had a 200 mm thickness and was reinforced
132 with a double layer of HD12 spaced at 225 mm. Wall 4 was reinforced with a double layer of reinforcing
133 bars to replicate the detailing commonly used in New Zealand. Wall 5 had the same geometry and
134 reinforcement detailing as for Wall 1 but was tested with the application of a moderate axial load of
135 $0.05A_g f'_c$. Similarly, Wall 6 and Wall 7 were intended to represent wall panels in the lower levels of
136 multi-storey buildings, which usually have a height to length aspect ratio of less than 3 and a moderate
137 level of axial load. These wall panels had a height to length aspect ratio of 2 and were tested with the
138 same level of axial load as was applied to Wall 5. The connection in Wall 7 was confined with the
139 placement of rectangular stirrups around the metal ducts, and for all tested wall panels the vertical and
140 horizontal reinforcement was anchored at the edges of the wall panel with a 90° standard hook.

141 To connect the wall panel to the foundation, starter bars from the foundation were embedded inside
142 600 mm long metal ducts that were later filled with non-shrinkage grout. The other end of the
143 connection reinforcement was anchored inside the foundation using a 90 degree standard hook. The
144 wall panel was initially erected on top of the foundation by providing a 20 mm gap underneath the
145 panel. The area around the gap was dry-packed and a day later was filled by pumping non-shrinkage
146 grout into the metal ducts.

147 **Test setup**

148 Two different test setups were used for testing the wall panels. For test specimens without applied axial
149 load, the test setup primarily consisted of a reinforced concrete footing, a precast concrete wall panel,
150 and a horizontally mounted hydraulic actuator providing the horizontal cyclic lateral force. The
151 movements of wall panels were restrained in their out-of-plane direction by two parallel H shape steel
152 columns that were positioned on each side of the wall panel. The details of the test setup are shown in
153 Fig. 4a. Both sides of the gap between the H shape steel columns and the loading beam were lubricated
154 with oil to minimize friction forces.

155 A different test setup was used in the experiments where axial load was applied, as the application of
156 axial load was achieved using two post-tensioned bars that were placed on each side of the wall panel.
157 During each of these latter experiments the bar force was adjusted to keep the applied axial force to
158 within $\pm 5\%$ of the target force. The post-tensioned bars were connected to a beam that was placed
159 perpendicularly on top of the steel I section beam positioned on top of the wall panel, and a pivot was
160 used between two beams in order to prevent application of any out-of-plane moments to the wall panel.
161 Two channel section beams were installed on each side of the wall panel in order to prevent out-of-
162 plane wall panel movement. One end of the beams was connected to the strong wall and the other end
163 was connected to a column placed at the other end of the wall panel. The beams restrained movement
164 of wall panels in their out-of-plane direction. The details of the second test setup are shown in Fig. 4b.

165 **Instrumentation**

166 The layout of instrumentation is shown in Fig.5. The walls were instrumented to monitor important
167 aspects of wall panel response when subjected to in-plane lateral loads, with the lateral load measured
168 by a load cell placed in series with the actuator. Two additional load cells were installed between the
169 post-tensioned bars and the strong floor to measure the applied axial load, and the lateral displacement
170 at the top of the wall panels was measured by a string potentiometer. To measure the lateral drift of
171 post-tensioned bars during testing of Panel 5 another string potentiometer was used to monitor the lateral
172 displacement that occurred at the top of the post-tensioned bars due to movement of the wall panel.
173 Because the magnitude of this displacement was found to be negligible, a decision was made to not
174 measure this displacement during the final two experiments. In-plane rocking deformations of the wall
175 panels were measured using three displacement gauges that were positioned at the two ends and at the
176 middle of the connection between the wall panel and the foundation. In addition, the relative in-plane
177 sliding displacement between the wall panel and foundation was monitored by a displacement gauge
178 and a LVDT installed midway along the connection. Shear and flexural deformations of the wall panels
179 were measured by 16 displacement gauges installed on each wall panel, and two displacement gauges
180 were used to measure sliding and uplift of the foundation relative to the laboratory strong floor.

181 Embedded strain gauges were utilized in each wall panel to measure reinforcement strains at critical
182 locations, with the pattern of embedded strain gauges shown in Fig. 5. Three reinforcement strain
183 gauges were positioned at the bottom, middle and top of the two outside connection bars extending
184 from the foundation, at elevations of 20 mm, 200 mm, and 400 mm above the connection level. In
185 addition, three reinforcement strain gauges were placed on the two outermost vertical bars of each wall
186 panel. In the wall panels where confinement reinforcement was provided to the connection, two
187 additional reinforcement strain gauges were attached to the bottom stirrups that confined the two
188 extreme connection bars, as shown in Fig. 5. In addition, two concrete strain gauges were positioned at
189 heights of 150 mm and 350 mm above the base of each wall.

190 **Material properties**

191 Concrete and steel reinforcement samples were taken during construction of the wall panels and grout
192 samples were collected during grouting of the connections. The reinforcement samples were tested by
193 applying monotonic axial tensile loads to the samples. Three grout cube samples with dimensions of
194 50×50×50 mm were tested for each wall panel. In addition, three concrete compression tests were
195 performed on cylinder samples with a radius of 100 mm and a height of 200 mm. Concrete samples
196 were subjected to similar curing conditions as for the wall panels by placing them next to each wall
197 panel. The grout samples were kept inside a plastic bag to emulate the condition of the utilised grout
198 inside the metal ducts. Grout and concrete samples were tested on the same day as the wall panel was
199 tested. The measured material strengths are summarised in Table 2.

200 **Testing procedure**

201 A loading protocol based on the ACI ITG-5.1 recommendations (ACI 2008) was used to determine the
202 applied loading sequence. The loading started with three force-controlled loading cycles and continued
203 with a series of displacement-controlled loading cycles until failure. The force at the first three force-
204 controlled cycles was below 0.6 of the nominal connection strength according to ACI ITG-5.1
205 recommendations (ACI 2008). The failure point was defined as the point where the stiffness had
206 decreased to less than 10% of the initial stiffness or the lateral force had decreased to 80% of the

207 maximum lateral force. Three cycles to the selected drift value were applied at each stage of the
208 displacement-controlled loading with the selected displacement-controlled drift values being 0.15%,
209 0.2%, 0.25%, 0.35%, 0.5%, 0.75%, 1.0%, 1.5%, 2.0%, 2.5%, and 3.5%. Because the loading was quasi-
210 static the impact forces resulted from wall panel movement were not considered in this experiment
211 programme.

212 **EXPERIMENTAL RESULTS**

213 **General response**

214 The behaviour of the wall panels varied dependent on the wall panel height to length aspect ratio and
215 the magnitude of axial load applied to each wall panel. The crack patterns of the seven tested wall panels
216 are shown in Fig. 6 and Fig. 7 and a summary of observed behaviour during the experiments is also
217 reported in Table 3. A summary of observed response of Wall 1-4 are presented below:

- 218 • Walls 1-3 behaved similarly, with their behaviour dominated by wall panel rocking on the
219 foundation, and noticeable sliding was also observed at the wall panel base. The different
220 detailing of connection confinement reinforcement did not affect the overall behaviour of walls
221 1-3. In each case the connection reinforcement fractured during cycles to 2.5% drift at which
222 point testing was concluded. No significant concrete spalling or crushing was observed in each
223 of the three tested wall panels.
- 224 • At a drift level of 2% different crack patterns were observed across the three wall panels, with
225 this variation being attributed to differences in the extent of out-of-plane displacement that
226 developed at the base of each panel. For each test this out-of-plane displacement was attributed
227 to a combination of bond slip and plastic deformation of the connection reinforcement as a gap
228 opened between the wall panel and the foundation during loading of the connection in tension.
229 During reversed loading this gap facilitated out-of-plane deformation at the base of the wall
230 panel when the connection was loaded in compression, with the different extents of out-of-
231 plane displacements resulting in different crack patterns on the three wall panels.

232 • the overall response of Wall 4 was dominated by rocking and wall panel sliding, and the panel
233 remaining undamaged during testing of Wall 4. The experiment concluded at a drift level of
234 between 2.0% and 2.5% when two of the outer connection bars fractured.

235

236 **The effect of axial load**

237 The application of a moderate level of $0.05A_g f'_c$ axial load to Wall 5-7 changed the performance of wall
238 panels in terms of extend of wall panel sliding, concrete spalling, and the failure type. The summary of
239 observed response of Wall 5 is presented below:

- 240 • The overall response of Wall 5 was dominated by rocking, but fewer cracks appeared in the
241 Wall 5 panel when compared to Wall 1 as the applied axial load prevented the formation of
242 cracking.
- 243 • In comparison with the previous four experiments, less wall panel sliding was measured. This
244 was attributed to axial load being applied to the wall panel, which contributed to closing of the
245 gap between the wall panel and foundation and resulted in increased friction being developed
246 along the connection between the wall panel and the foundation.

247

248 **The effect of wall panel length**

249 The length of wall panels affected the failure mechanism of the wall panels with grouted metal duct
250 connections. The increase of wall panel length increases the length of compression toe of the and may
251 resulted in metal duct pull out from the wall panel. As a result, different performance was observed for
252 Wall 6, which had a larger length than for the previous five wall panels (see Table 1). The summary of
253 observed response of Wall 6-7 is presented below:

- 254 • More extensive concrete spalling was observed for Walls 6 and 7 than for the previous five
255 experiments. The reason for this behaviour was attributed to the larger axial load applied to

256 Walls 6 and 7 and the lower height to length ratio of these two wall panels, which resulted in a
257 larger compression force acting at the wall panel toes.

258 • The extensive concrete damage at a drift level of 1.5% caused the outermost metal duct to be
259 exposed and subsequently be pulled out of the wall panel as the connection splice failed , as
260 shown in Fig. 8a.

261 • The wide cracks and more extensive concrete spalling observed in Wall 6 demonstrated the
262 larger contribution of the wall panel flexural deformation to the overall response of Wall 6 in
263 comparison with the previous five tests.

264 • Concrete spalling occurred in smaller area in Wall 7 in comparison with Wall 6 due to both the
265 confinement reinforcement that ensured that the splice was maintained and the increased
266 vertical reinforcement that supported the confinement reinforcement, as shown in Fig. 8b.
267 Testing concluded at a drift level of 1.5% after the outermost connection reinforcement
268 fractured at both ends of the wall panel.

269

270 **Comparison with monolithic shear walls**

271 All seven tested wall panels experienced less damage than expected for conventional monolithic
272 reinforced concrete walls, and most of the damage was concentrated in the connection region. Excluding
273 panel uplift, the width of cracks in the panel was less than 4 mm in all experiments, and concrete
274 crushing was much less than typically observed for comparable (lightly reinforced) flexure controlled
275 reinforced concrete walls (Lu et al. 2016). This difference was more obvious in Wall 4 because of the
276 larger wall panel flexural strength in comparison with its connection strength, which is typical of jointed
277 precast panel designs.

278 **The effect of connection confinement**

279 The influence of connection confinement on wall panel behaviour was found to be significantly
280 dependent on the magnitude of compression stress at the wall panel toe. When the compression stress
281 was large enough to cause substantial concrete spalling at the corners of wall panels, the use of confining

282 stirrups improved the connection performance and prevented spalling around the metal duct and
283 associated degradation of the splice between the wall panel and the connection reinforcement, leading
284 to the full capacity of the connection being achieved. In contrast, no significant difference in
285 performance was observed when the confining stirrups were used in wall panels that had a smaller wall
286 panel length and no additional axial force applied.

287 **Force-displacement behaviour**

288 The resultant force-displacement hysteresis responses for Wall 1 to Wall 4 are shown in Fig. 9. The
289 behaviour of the four wall panels was very similar as their connection characteristics and subsequent
290 failure modes were the same. During the first three forced-controlled loading cycles the wall panels
291 were effectively elastic, whilst in the fourth cycle a nonlinear response was observed due to the
292 commencement of both panel cracking and yielding of the wall-foundation connection reinforcement.
293 In the following cycles a gap opened at the bottom of each of the four tested wall panels, causing
294 pinching of the force-displacement response. This behaviour was due to the gap opening in the
295 connection zone which decreased the stiffness of the wall panels because the moment was carried by
296 only the connection reinforcement. Finally, all four tests were concluded when the connection
297 reinforcement fractured, causing rapid strength degradation. The four wall panels had similar maximum
298 lateral strengths of approximately 53 kN, and in all four wall panels the maximum measured lateral
299 force was larger than the calculated nominal strength of the panel-foundation connection which was
300 equal to 46 kN for Wall 1 to Wall 3, and 47 kN for Wall 4. All four wall panels achieved a drift capacity
301 of 2% prior to fracture of the connection reinforcement.

302 The obtained force-displacement response for Wall 5 is shown in Fig. 10a. The wall panel behaved
303 linearly during three force-controlled cycles, and in the next cycle yielding of the connection
304 reinforcement commenced. At larger drift levels the hysteretic response began to display nonlinear
305 behaviour, with larger residual displacement due to wall panel cracking and plastic deformation of the
306 connection reinforcement. The magnitude of residual displacement was less than that measured during
307 testing of Walls 1-4 due to fewer cracks forming in the wall panel and smaller gap opening at the

308 connection, attributed to the increased magnitude of applied axial load. When the 2.0% drift level was
309 applied to the wall panel the lateral force reached the maximum recorded magnitude of 110 kN and at
310 the next drift level of 2.5% more extensive cracking and concrete spalling occurred, leading to a
311 reduction in wall panel stiffness, with the lateral force dropping to a magnitude of 75 kN (68% of the
312 peak strength). Testing was concluded by applying a 3.5% drift level that caused fracture of the
313 connection reinforcement. This reinforcement fracture occurred at a larger drift level than in the
314 previous four experiments due to the reduced extent of gap opening at the connection and consequently
315 smaller strains in the connection reinforcement for a given drift level. The maximum lateral force
316 measured in this test was approximately twice the magnitude measured in the previous four experiments
317 due to the larger axial load applied to the wall panel. The lateral strength of Wall 5 was also larger than
318 the corresponding calculated lateral force for nominal flexural strength of the wall panel connection
319 (87 kN). The other difference between this experiment and the earlier wall panel tests was that the
320 unloading curve was less steeply inclined than for the four previous tests, causing smaller residual
321 displacement at each cycle. In addition, there was less pinching of the force-displacement diagram for
322 Wall 5 than for the previous four experiments. The reason for the differences in hysteretic response of
323 Wall 5 in comparison to the previous four experiments was again attributed to the application of axial
324 compression to the wall, which helped to close the wall-to-foundation joint when unloading.

325 In Fig. 10b and Fig. 10c the force-displacement response of Wall 6 and Wall 7 are shown. Larger lateral
326 strengths were measured in these wall panels when compared with the previous five tests, due to the
327 greater dimensions of the wall panels and the larger value of the axial load. At drift levels below 1.5%
328 the behaviour of Wall 6 and of Wall 7 were almost identical, with peak lateral strengths reaching similar
329 magnitudes of 308 kN for Wall 6 and 307 kN for Wall 7, although these peak strengths occurred at
330 differing drift levels of 1.5% for Wall 6 and of 1.0% for Wall 7. The reason for the different drift
331 capacity between the two experiments was attributed to the different failure mode in each experiment.
332 Failure of Wall 6 was due to progressive concrete spalling which resulted in the metal duct becoming
333 detached from the wall panel, as shown in Fig. 8a. In contrast the failure of Wall 7, which had more

334 robust splices between the connection reinforcement and the vertical reinforcement of the wall panel,
335 was due to fracture of the connection reinforcement.

336 The back-bone force-displacement responses extracted from the first cycle to each drift level for each
337 of the seven experiments are compared in Fig. 11. In order to eliminate the effects of the different wall
338 panel lengths and heights the ratios of measured lateral force to calculated nominal strength of the
339 connections were plotted versus the magnitude of drift level, to reveal that the backbone curves of all
340 wall panels were similar. It was also found that the last three tested wall panels, where axial load was
341 applied, had larger margins above the normalized nominal strength than for the other four experiments.

342 **Deformation components**

343 The contributions of the four in-plane mechanisms consisting of rocking, sliding, flexure, and shear
344 deformation were measured in all experiments by using displacement gauges that were positioned on
345 the wall panels and their connections to the foundation. Flexural deformations were obtained by
346 measuring the rotation of the wall panel horizontal cross sections as proposed by Hiraishi (1984) and
347 shear deformations were obtained using diagonal displacements, again based upon a previously
348 proposed method (Hiraishi 1984) which considered the influence of flexural deformation on the
349 measured diagonal displacements. The extent of wall panel rocking was calculated according to the
350 uplift measured by two displacement gauges positioned at the extreme edges of the wall panel and
351 sliding was obtained directly by a displacement gauge and an LVDT that were installed at the middle
352 of the wall panel connection with the foundation. The sum of the four displacement mechanisms was
353 compared with the measured displacement at the top of the wall panels and the difference between these
354 two values indicated the measurement error, which was less than 10% for all seven tests. The
355 contributions of each force-displacement mechanism to the overall response of the seven wall panels
356 are shown in Fig. 12 and Fig. 13.

357 In general, the response of Walls 1-4 was dominated by rocking at the wall-to-foundation interface,
358 contributing to between 69-90% of the total lateral displacement during larger drift cycles. The flexural
359 deformation of Wall 1 was approximately 15% of the overall displacement when the connection

360 reinforcement was below the yield stress, but at larger drift levels yielding of the connection
361 reinforcement resulted in a gap opening at the connection that facilitated rocking and sliding of the wall
362 panel. Sliding displacements contributed more than flexural displacements to the total response of the
363 wall panel at larger drift levels. Shear deformation had a negligible contribution to the force-
364 displacement behaviour of Wall 1. A similar behaviour was observed for Wall 2 and Wall 3 but the
365 contribution of rocking in Wall 4 was larger than for the previous three experiments because Wall 4
366 had a greater thickness and greater vertical reinforcement content, which limited both the flexural and
367 shear deformations of the wall panel.

368 The contribution of rocking to the overall response of Walls 1-4 was larger than for Walls 5-7. The
369 reason for this response was that the absence of applied axial load for Walls 1-4 facilitated rocking and
370 limited the extent of concrete spalling, consequently decreasing the flexural deformation of these wall
371 panels when compared to Walls 5-7. The contributions of sliding and rocking in Wall 5-7 were lower
372 due to the application of axial load.

373 In Wall 6 and Wall 7 the flexural deformations of the wall panels had a greater contribution in
374 comparison to the behaviour observed in the previous five tests. The increased flexural deformations
375 were attributed to the increased panel dimensions and increased axial load, which resulted in increased
376 panel cracking and spalling. Wall panel flexural deformation provided the largest contribution to the
377 lateral displacement for Wall 6, whilst in Wall 7 panel rocking was more dominant. The larger
378 contribution of flexural deformation in Wall 6 correlated with the observed increase in panel crack
379 widths and spalling when compared to Wall 7 where the panel and connection splice remained less
380 damaged and instead the wall panel rocked about the wall base.

381 **Energy dissipation**

382 In the displacement-based seismic design method the determination of equivalent viscous damping
383 (EVD) is required. The EVD can be calculated by:

$$384 \quad \xi = \frac{A_h}{2\pi\Delta_m F_m} \quad (1)$$

385 where ξ is equivalent viscous damping, A_h is the enclosed area of each cycle of the force-displacement
386 diagram, Δ_m is the maximum displacement in a cycle, and F_m is the maximum lateral force in a cycle.
387 The calculated EVD for the first cycle of each drift level for all wall panels is shown in Fig. 14. All wall
388 panels had lower EVD when compared with commonly adopted values for monolithic reinforced
389 concrete walls, which are typically greater than 20% at the failure cycle for wall panels subjected to
390 moderate level of axial load and greater than 25% for wall panels having no applied axial load (Lu et
391 al. 2016, Zhang and Zhihao 2000). The reason for this reduced level of EVD, when compared with
392 comparable monolithic construction, was attributed to the reduced extent of plastic deformations, which
393 mostly developed in the connection zone rather than as distributed plasticity associated with a traditional
394 plastic hinge region at the base of the wall. The EVD increased as greater drift levels were applied to
395 the wall panel up to a drift level of 1.5%, because at larger drift levels a larger extent of plastic
396 deformation of the connection reinforcement and more extensive concrete cracking occurred than at
397 smaller drift levels. In all experiments the EVD reached a peak value at a drift level of 1.5% and then
398 reduced as larger drift levels beyond 1.5% were applied to the wall panels. This behaviour was mainly
399 because of greater pinching of the force-displacement diagram at larger cycles that was attributed to a
400 combination of bond slip and plastic deformation of the connection reinforcement as a gap opened
401 between the wall panel and the foundation.

402 Wall 1 to Wall 4 had larger EVD than for the other three tested wall panels because no axial load was
403 applied to these walls, resulting in a fatter hysteresis response. Walls 5-7 had lower EVD than for the
404 previous four experiments because the applied axial load resulted in a more steeply inclined unloading
405 force-displacement curve and an associated reduction in the enclosed area of each cycle. The EVDs of
406 Wall 6 and Wall 7 were approximately the same when the applied drift level was below 1.5%, but the
407 EVD of Wall 6 reduced at higher drifts due to splice degradation and disconnection of the two outermost
408 reinforcing bars that caused a reduction in the capacity of the wall panel to dissipate energy.

409 CONCLUSIONS

410 The cyclic response of precast concrete wall panels with grouted metal duct connections representative
411 of those commonly used in existing buildings was examined, focusing on parameters such as applied
412 axial load level, wall panel geometry, and varying detailing of the splice confinement between the wall
413 panel and connection reinforcement. The following conclusions were drawn:

- 414 • The overall behaviour of all seven wall panels was consistent with the design philosophy for
415 precast concrete panels having equivalent monolithic connections. The wall panel stiffness and
416 nonlinear behaviour were consistent with that of monolithic concrete walls.
- 417 • The measured lateral strength of all wall panels was larger than their calculated nominal
418 strength, and in most cases the full capacity of the connection was achieved prior to failure.
419 Despite the low drift capacity of some walls, the test results confirmed that walls having metal
420 duct connections in existing buildings that were designed for nominally ductile actions are
421 likely to have adequate seismic strength.
- 422 • Due to the increased ratio of panel strength to connection strength, the behaviour of the wall
423 with a double layer of reinforcement was dominated by rocking about the wall base, with no
424 cracking in the panel itself. Rocking was found to contribute less to lateral deformation for the
425 wall panels having a single layer of reinforcement because of flexural deformations due to panel
426 cracking.
- 427 • For short wall lengths and low axial loads, panel failure was controlled by fracture of the
428 connection reinforcement. For the longer wall panel with larger axial load and no confinement
429 reinforcement, concrete spalling resulted in the metal duct becoming detached from the wall
430 panel when the compression strain at the wall panel compression toe was large enough to cause
431 extensive concrete spalling. This type of failure is more likely to occur in wall panels with a
432 larger length, greater connection reinforcement content, and a greater magnitude of applied
433 axial load.

- 434 • The measured compression strain at the wall panel toes prior to spalling was approximately
435 0.002, which is significantly less than typical concrete failure strains. This small failure strain
436 highlights the lack of robustness of singly reinforced walls with no confinement reinforcement.
- 437 • The use of transverse reinforcement in the form of stirrups to confine the connection
438 reinforcement and a larger quantity of vertical reinforcement around metal ducts increased the
439 strength and ductility of the wall panel toe, limiting the concrete spalling and preventing failure
440 of the metal duct connection by reinforcement pull-out. However, the use of confinement
441 stirrups did not increase the drift capacity of the wall panels, with the failure mode shifting to
442 reinforcement fracture due to concentrated rocking about the wall base. In the walls where
443 spalling of the wall panel toe did not occur, the influence of the stirrups on the connection
444 performance and overall behaviour of the wall panels was insignificant.

445 **ACKNOWLEDGEMENT**

446 This research was funded by the New Zealand Natural Hazard Research Platform (NHRP) and the
447 Building Systems Performance branch of the Ministry of Business, Innovation and Employment
448 (MBIE). In addition, the authors would like to acknowledge the project management support and
449 coordination from the UC Quake Centre. Materials, construction of specimen and general advice were
450 provided by Concretec New Zealand Ltd, Precast New Zealand, and Sika New Zealand Ltd, and their
451 contributions are gratefully acknowledged. The authors also wish to acknowledge the contributions of
452 Jay Naidoo, Andrew Virtue, Mark Byrami, Shane Smith, Ross Reichardt, and Jerome Quenneville who
453 assisted with the testing of the wall panels in the Structures Testing Laboratory at the University of
454 Auckland. This project was partially supported by QuakeCoRE, a New Zealand Tertiary Education
455 Commission-funded Centre. This is QuakeCoRE publication number 0158.

456 **REFERENCES**

457 ACI Innovation Task Group 5. (2008). “Acceptance criteria for special unbonded post-tensioned precast
458 structural walls based on validation testing and commentary (ACI ITG-5.1 M-07).” *American Concrete*
459 *Institute*, Farmington Hills, MI.

460 Becker, J. M., Llorente, C., & Mueller, P. (1980). "Seismic response of precast concrete walls."
461 *Earthquake Engineering & Structural Dynamics.*, 8(6), 545-564.

462 Crisafulli, F. J., Restrepo, J. I., & Park, R. (2002). "Seismic design of lightly reinforced precast concrete
463 rectangular wall panels." *PCI Journal.*, 47 (4), 104-121.

464 Hawkins, N. M., & Englekirk, R.E. (1987). "US-Japan seminar on precast concrete construction in
465 seismic zones." *PCI Journal.*, 32(2), 75-85.

466 Hiraishi H (1984). "Evaluation of shear and flexural deformation of flexural type shear walls." *Bulletin*
467 *of the New Zealand National Society for Earthquake Engineering.*, 17 (2), 135-144.

468 Kim, Y. M. (2000). *A study of pipe splice sleeves for use in precast beam-column connections.* Master's
469 thesis, University of Texas at Austin.

470 Lu, Y., Henry, R. S., Gultom, R., & Ma, Q. T. (2016). "Cyclic testing of reinforced concrete walls with
471 distributed minimum vertical reinforcement." *Journal of Structural Engineering*, 04016225.

472 Standards Association of New Zealand, (2004). "NZS 1170.5: Structural design actions. Part 5:
473 Earthquake actions – New Zealand." *Standards New Zealand*, Wellington.

474 PCI Industry Handbook Committee (2010). "PCI design handbook: precast and prestressed concrete."
475 *Prestressed Concrete Inst*, 7th Edition, Chicago, IL.

476 Restrepo, J. I., Tobolski, M. J., & Matsumoto, E. E. (2011). "Development of a precast bent cap system
477 for seismic regions." *National Cooperative Highway Research Program*, Report 681.

478 Riva, P. (2006). "Seismic behaviour of precast column-to-foundation grouted sleeve connections." *In*
479 *Proceeding of the International Conference on Advances in Engineering Structures.*, Mechanics &
480 Construction, Waterloo, Ontario, Canada, 121-128.

481 Seifi, P., Henry, R. S., & Ingham, J. M. (2016). "Panel connection details in existing New Zealand
482 precast concrete buildings." *Bulletin of the New Zealand Society for Earthquake Engineering.*, 49(2),
483 190-199.

484 SESOC Interim Design Guidance (2013). “Design of conventional structural systems following the
 485 Canterbury earthquakes.” *Structural Engineering Society of New Zealand*, New Zealand.

486 Thonstad, T., Mantawy, I. M., Stanton, J. F., Eberhard, M. O., & Sanders, D. H. (2016). “Shaking table
 487 performance of a new bridge system with pretensioned rocking columns.” *Journal of Bridge
 488 Engineering*, 21(4), 04015079.

489 Zhang, Y, and Zhihao W (2000). “Seismic behavior of reinforced concrete shear walls subjected to high
 490 axial loading.” *ACI Structural Journal*., 97(5), 739-750.

491 **Table 1.** Details of the test wall panels

Wall panel number	Length (mm)	Height (mm)	Aspect ratio	Thickness (mm)	Connection reinforcement	Vertical reinforcement	Confining reinforcement	Axial Load (% $A_g f'_c$)
1	1000	3000	3	150	HD16@400	Single layer HD12@225	-	0
2	1000	3000	3	150	HD16@400	Single layer HD12@225	Spiral	0
3	1000	3000	3	150	HD16@400	Single layer HD12@225	Rectangular	0
4	1000	3000	3	200	HD16@400	Double layer HD12@225	-	0
5	1000	3000	3	150	HD16@400	Single layer HD12@225	-	5%
6	2000	4000	2	150	HD16@450	Single layer HD12@225	-	5%
7	2000	4000	2	150	HD16@450	Single layer HD12@225	Rectangular	5%

492 **Table 2.** Properties of utilized materials (all stresses in MPa units)

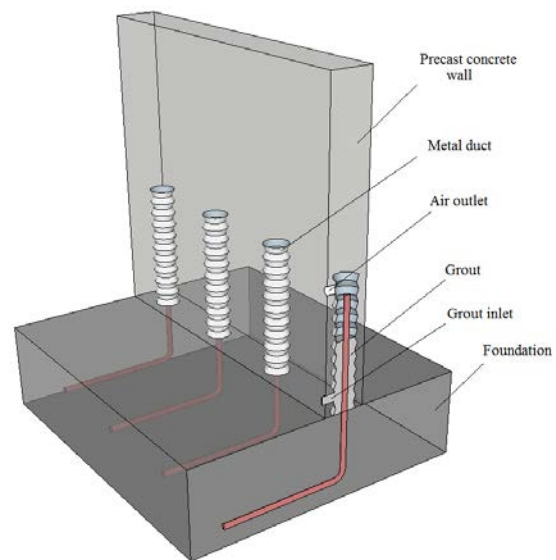
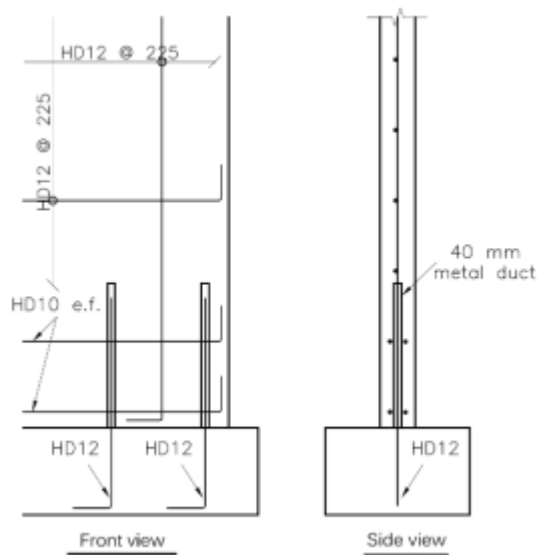
Wall panel number	Grout strength	Concrete strength	Connection reinforcement			Panel reinforcement		
			Yield stress	Ultimate stress	Strain at peak strength	Yield stress	Ultimate stress	Strain at peak strength
1	58	46	473	632	0.10	523	653	0.11
2	43	54	473	632	0.10	523	653	0.11
3	56	46	473	632	0.10	523	653	0.11
4	50	56	473	632	0.10	523	653	0.11
5	52	43	482	629	0.11	520	641	0.11
6	54	53	482	629	0.11	520	641	0.11
7	64	45	482	629	0.11	520	716	0.12

493 **Table 3.** Summary of observed crack widths and failure drifts

Wall panel number	Maximum wall panel crack width (mm)	Corresponding drift at maximum crack width (%)	Failure drift (%)	Maximum crack width at failure* drift (mm)	Wall panel uplift at failure* drift (mm)
1	1.4	2	1.8	1.0	25.0
2	1.6	2	2.1	1.0	25.0
3	0.4	2	2.0	0.2	27.2
4	0	2	2.0	0	25.6
5	1.8	1.5	2.1	0.4	17.8
6	4.0	1.5	1.5	0.5	**
7	3.0	1	1.2	1.4	19.2

494 * Failure was defined as drift at which either metal duct pull-out or reinforcement fracture occurred.

495 ** Wall panel uplift could not be measured due to extensive spalling.



(a) An example of a conventional metal duct wall-to-foundation connection detail

(b) Grouted metal duct connection (wall panel and foundation reinforcement not shown)

496

Fig. 1. Grouted metal duct connection details.

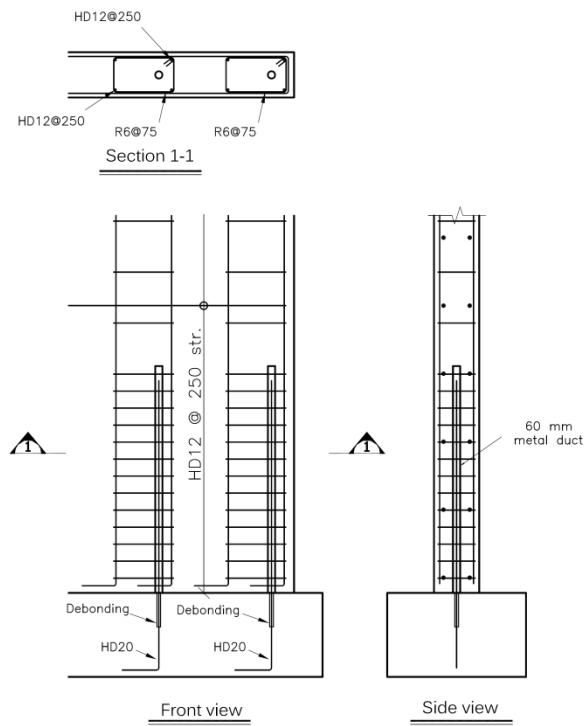


497

498 **Fig. 2.** An example of metal duct connection damage during the 2010/2011 Canterbury earthquakes.

499

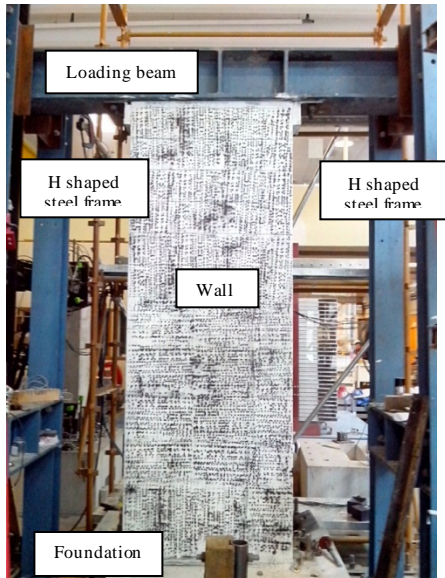
(Photo credit: Ken Elwood)



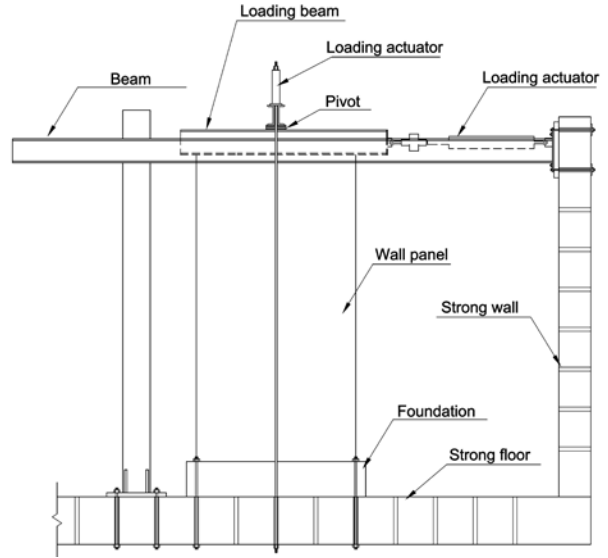
500

501 **Fig. 3.** An example of SESOC recommended detailing (SESOC 2013) for metal duct connections.

502



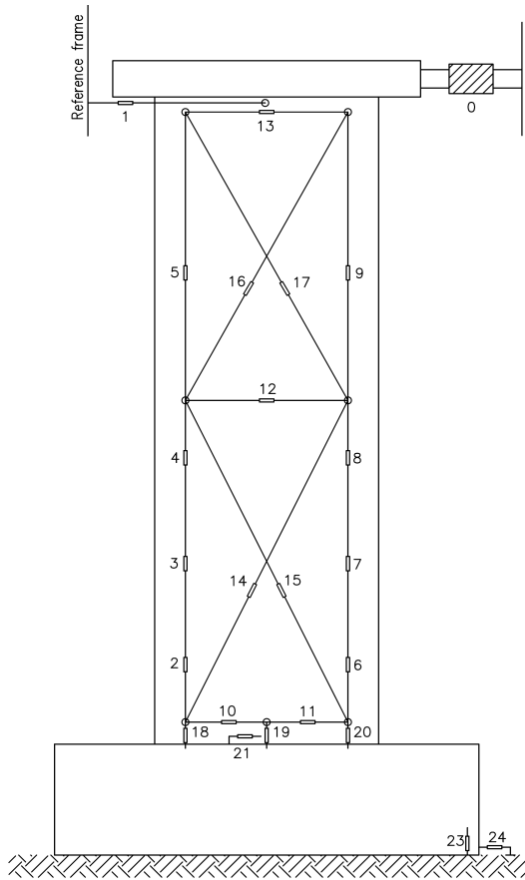
(a) Test setup without application of axial load



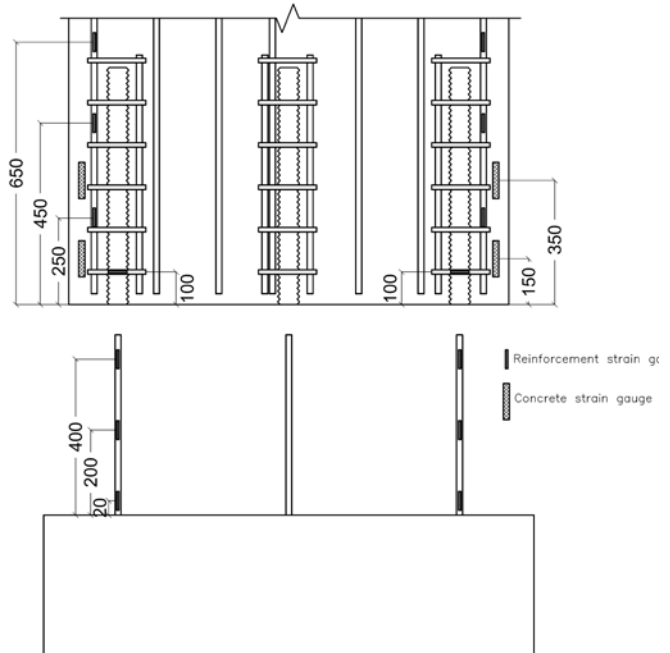
(b) Test setup with application of axial load

503

Fig. 4. Test setup



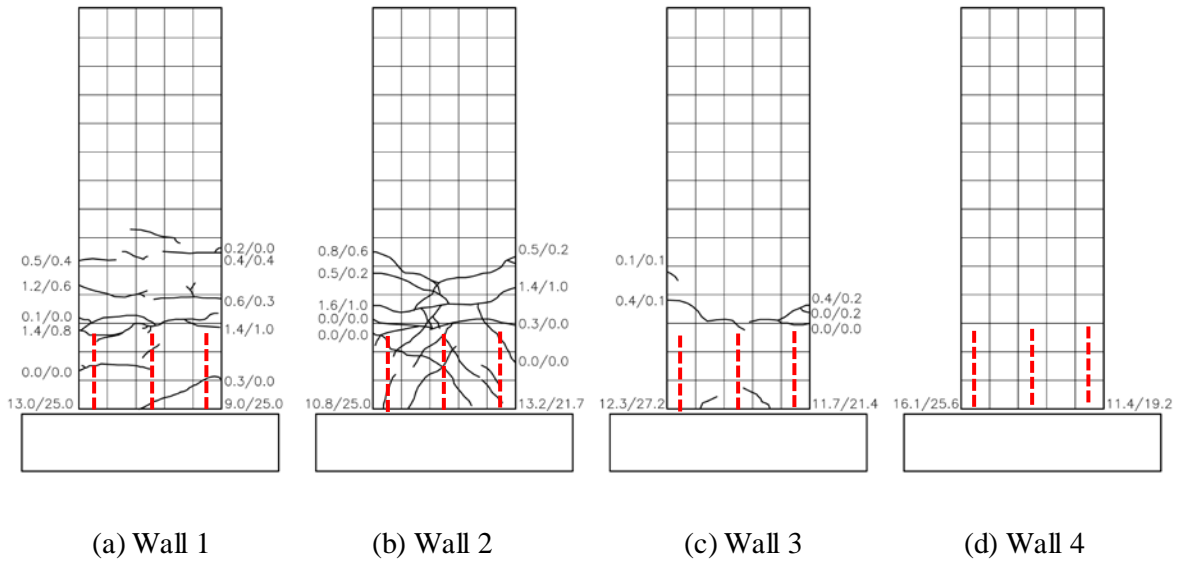
(a) Non-embedded instrumentation



* Not to scale; horizontal reinforcement not shown for clarity

(b) Distribution of embedded strain gauges

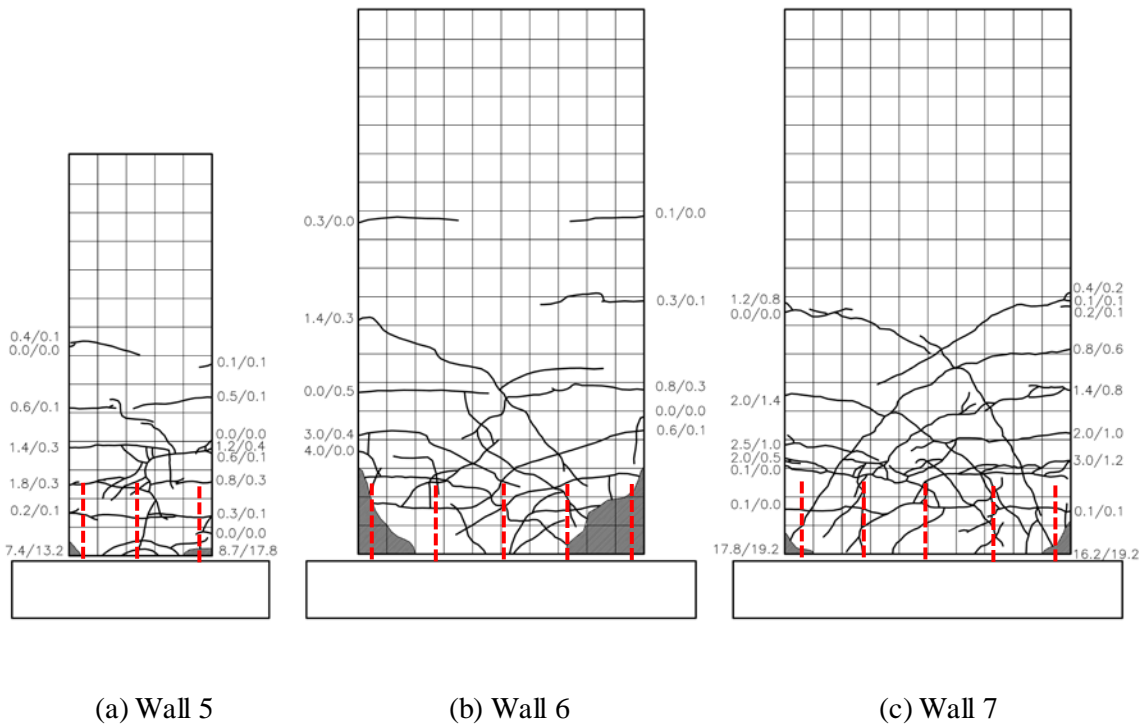
Fig. 5. Distribution of instrumentation (front view of wall panel)



* The connection reinforcement is shown with a dash line.

Fig. 6. Crack patterns for wall panels without application of axial load (dimensions refer to crack

width at maximum load/crack width at last cycle)



* The top of connection reinforcement is shown with a dash line.

507 **Fig. 7.** Crack patterns for wall panels with application of axial load (dimensions refer to crack width
508 at maximum load/crack width at last cycle)

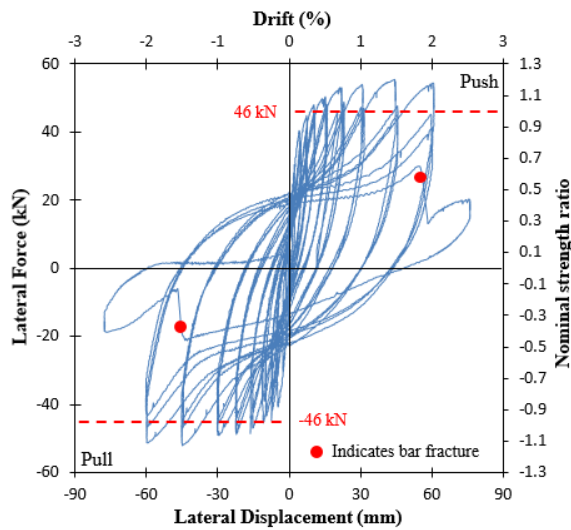


(a) Wall 6

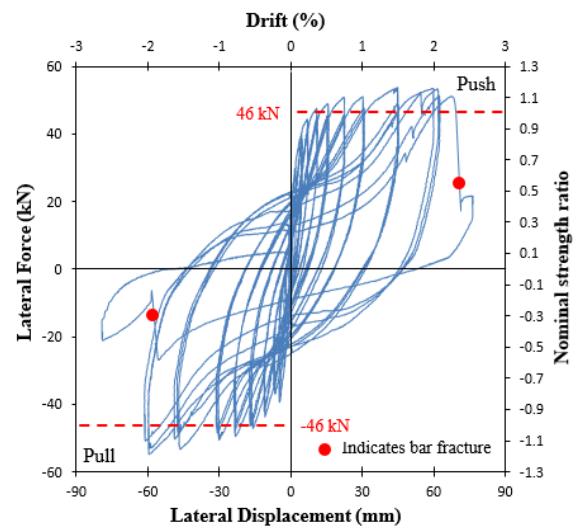


(b) Wall 7

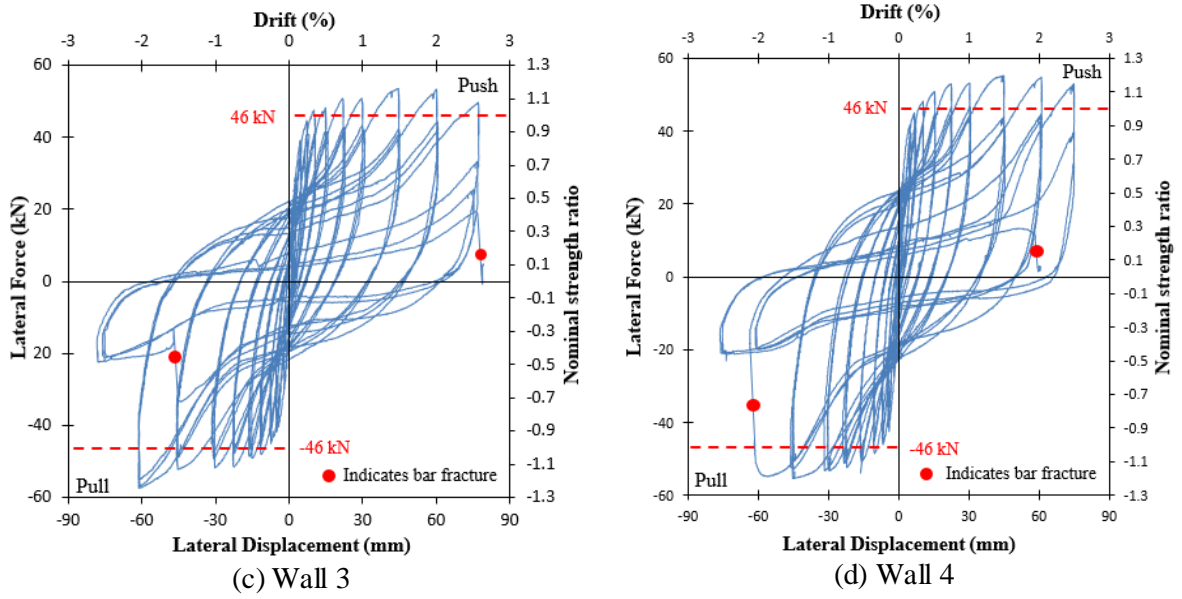
509 **Fig. 8.** Condition of compression zones of Wall 6 and Wall 7 at the conclusion of testing



(a) Wall 1

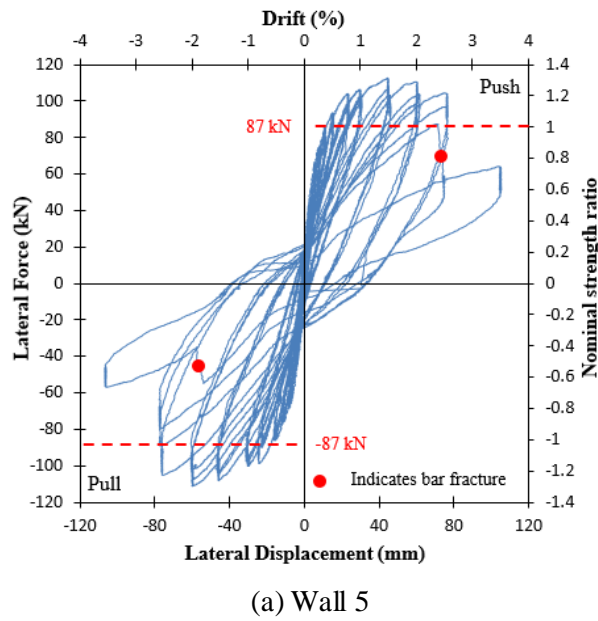


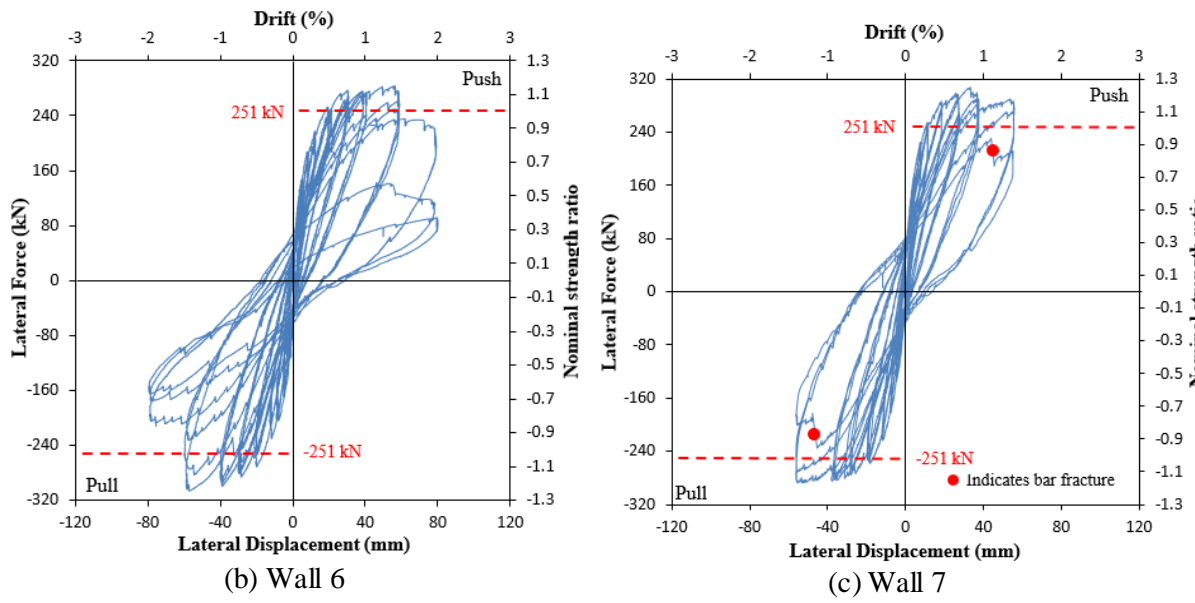
(b) Wall 2



510

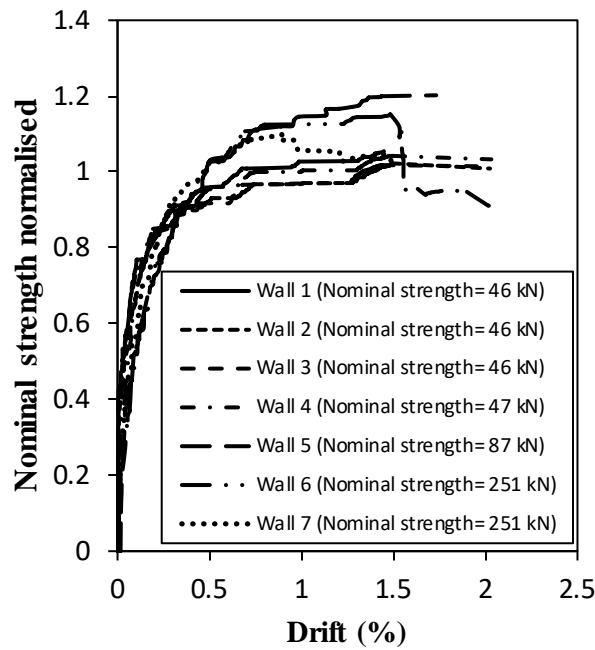
Fig. 9. Hysteresis response of wall panels with no applied axial load





511

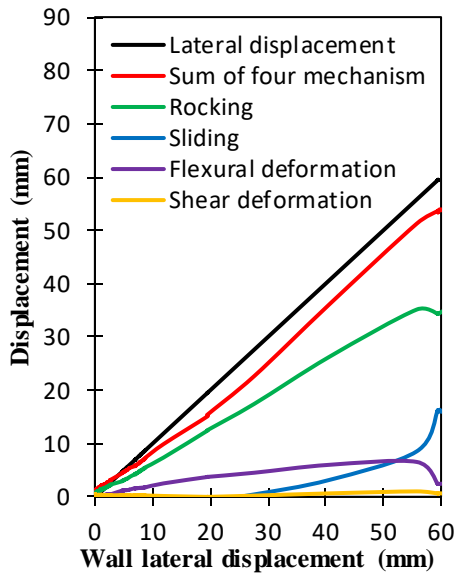
Fig. 10. Hysteresis response of wall panels with applied axial load



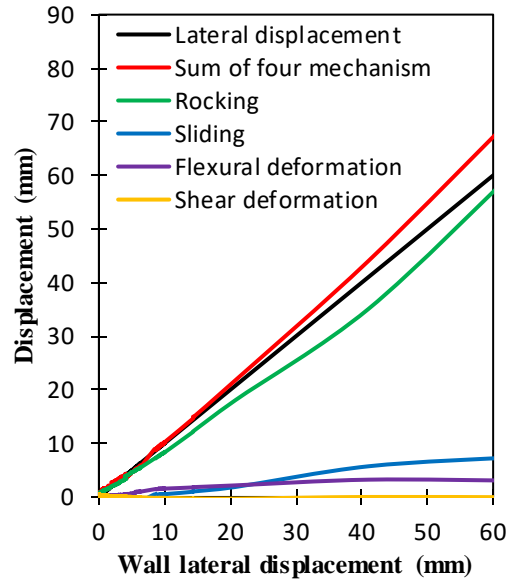
512

513

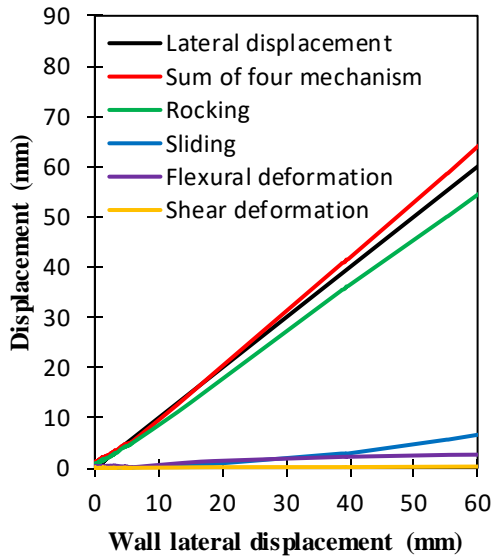
Fig. 11. Force-displacement backbone curves normalised against calculated nominal strength



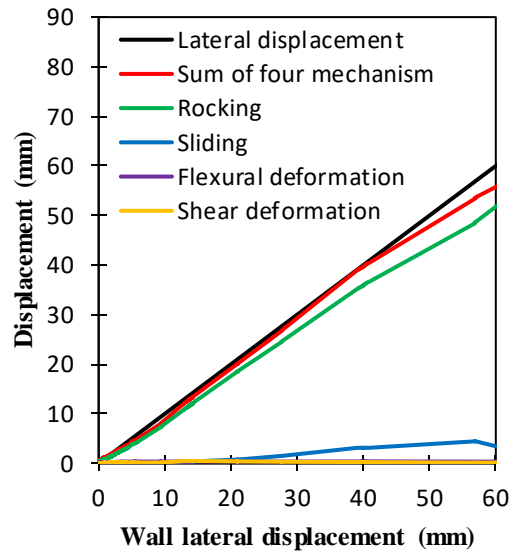
(a) Wall 1



(b) Wall 2

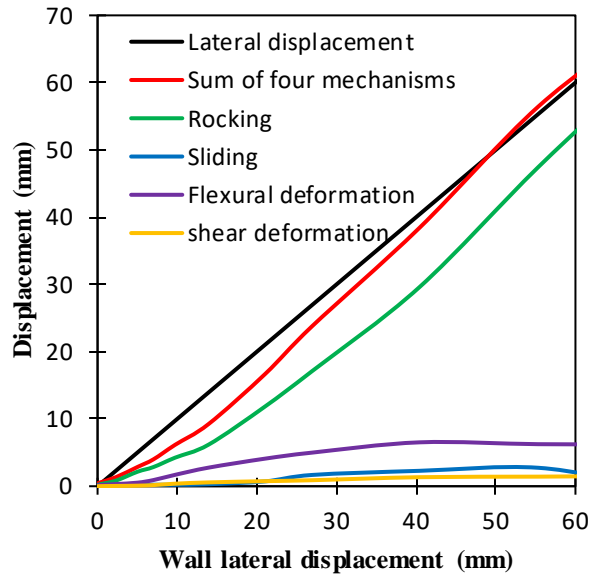


(c) Wall 3

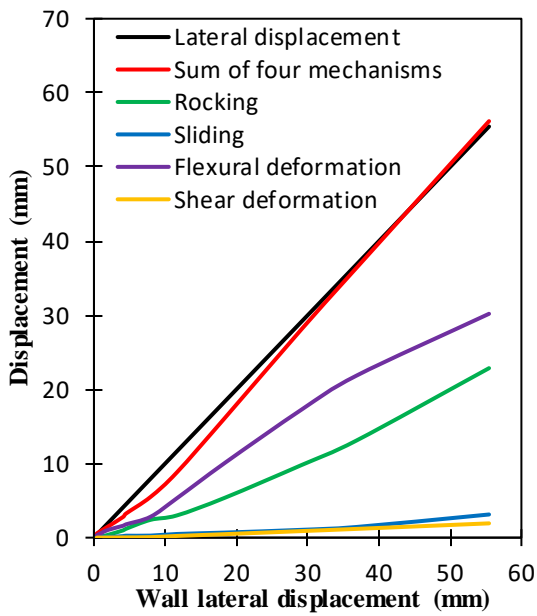


(d) Wall 4

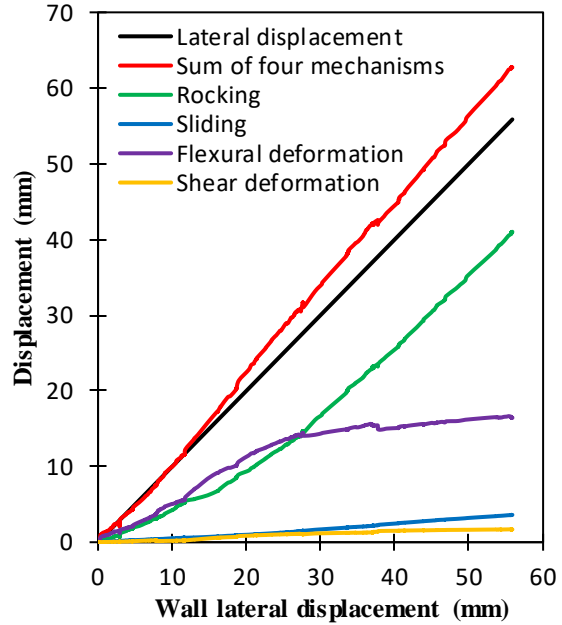
514 **Fig. 12.** Contribution of each deformation mode to overall response for wall panels with no applied
 515 axial load



(a) Wall 5

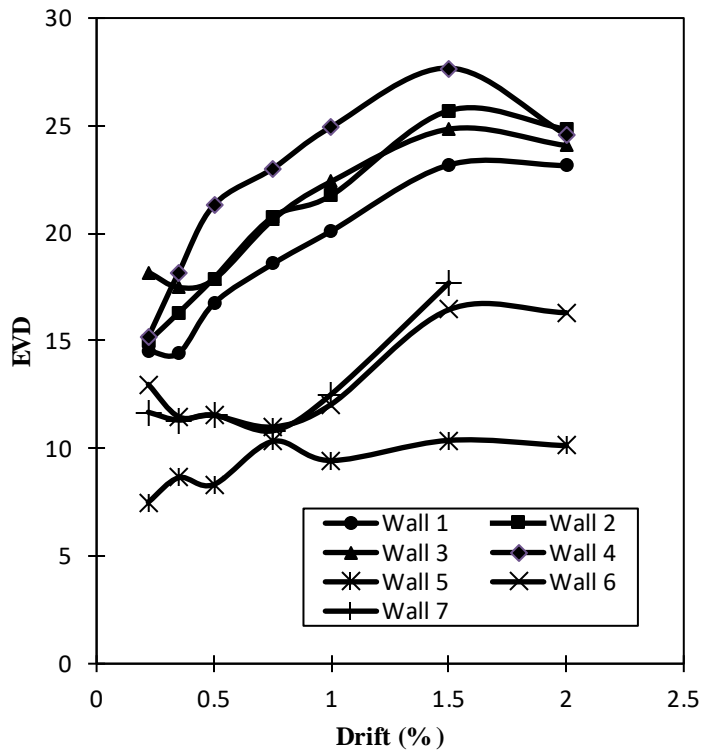


(b) Wall 6



(c) Wall 7

516 **Fig. 13.** Contribution of each deformation mode to overall response for wall panels with applied axial
 517 load



518

519

520

521

Fig. 14. Equivalent viscous damping of each wall panel